Chemically Etched Fiber-Waveguide Interface

1st Bernardo de A. Dias da Costa
Gleb Wataghin Institute of Physics
University of Campinas
Campinas, SP, Brasil
b250832@dac.unicamp.br

2nd Pedro V. Pinho
Gleb Wataghin Institute of Physics
University of Campinas
Campinas, SP, Brasil

3rd Lucas G. Woiblet
Gleb Wataghin Institute of Physics
University of Campinas
Campinas, SP, Brasil

4th Nick J. Schilder
Gleb Wataghin Institute of Physics
University of Campinas
Campinas, SP, Brasil

5th Antonio Von Zuben
Gleb Wataghin Institute of Physics
University of Campinas
Campinas, SP, Brasil

6th Gustavo S. Wiederhecker
Gleb Wataghin Institute of Physics
University of Campinas
Campinas, SP, Brasil

7rd Thiago P. Mayer Alegre
Gleb Wataghin Institute of Physics
University of Campinas
Campinas, SP, Brasil
alegre@unicamp.br

***Abstract*—We present a simple and effective method for fabricating chemically etched tapered fibers optimized for high-efficiency coupling with silicon integrated waveguides. The process involves immersing a stripped single-mode optical fiber in a 50% HF solution and gradually pulling the fiber as the acid etches its sides, resulting in a conical shape. This technique enables precise control over critical geometrical parameters, including the conical angle, tip diameter, and overall taper length. By fine-tuning these parameters, we can produce couplers with ideal geometries tailored to specific integrated photonic chips, thereby significantly improving coupling efficiency.**

***Index Terms*—Conical tapers, nanophotonics, optomechanics, coupling efficiency.**

I. Introduction

A critical challenge in integrated photonics is the efficient coupling of light between optical fibers and on-chip waveguides [1]. This is particularly crucial in quantum networks [2], where both high bandwidth and high fidelity are essential. The conventional optical fibers, with their larger mode diameters, have been found inadequate for this purpose, as a significant portion of the signal is lost before it can be effectively transmitted into the chip's waveguide. To address this bottleneck, different coupling techniques have been developed, such as loop taper [3], butt coupling [4] and nano-spikes [5].

In this work, we focus on the study of those nanometric conical optical fibers, or nanospikes. These fiber tapered couplers have recently attracted significant interest due to several advantages: flexibility, strong evanescent field, ease of fabrication, and high coupling efficiency, potentially reaching 99% of light transmission [6].

II. Adiabatic fiber-waveguide simulations

Our goal is to develop an optimized nano-spike for efficient coupling with a silicon inverted taper waveguide terminated by a photonic crystal mirror. The silicon waveguide is then used to evanescently couple to an optical or optomechanical resonator. Using finite element simulations on a commercial software (COMSOL Multiphysics) we determine the optimal geometries for the nano-spike. To characterize the coupling efficiency, we measured and calibrate the reflected signal coming from the silicon waveguide and compare with other systems.

A key criteria, or adiabatic condition, to achieve both low loss in the nano-spike and efficient coupling with the silicon waveguide, is to slowly vary each waveguide cross section along the propagation directions. This ensures minimal power loss due to scattering into undesired higher-order propagating modes or radiation modes of the nano-spike. The condition can be expressed as follows [7]:

$$L_{taper} \gg L_{beat} = \frac{\lambda}{n_{\text{eff},1} - n_{\text{eff},2}}, \tag{1}$$

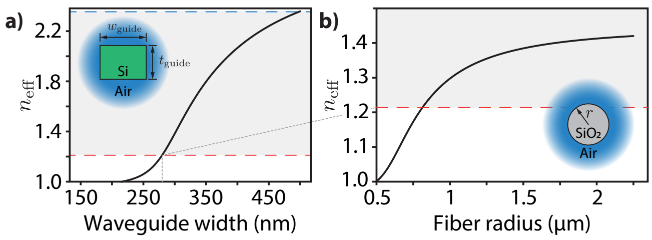

Fig. 1. Finite Element Method simulation of the effective refractive index (n_{eff}): **a)** Air-cladded rectangular silicon waveguide with varying width (w_{guide}) and a fixed height of t=220 nm. The shaded region represents the range of n_{eff} values along the tapered silicon waveguide. **b)** Air-cladded SiO_2 optical fiber with varying radius. The shaded region encompasses all possible n_{eff} values for the optical fiber's propagating mode, bounded by the n_{eff} of a silicon waveguide with a width of 280 nm.

where z_t is the transition length, z_{beat} is the beating length between two modes with effective refractive indices $n_{\text{eff},1}$ and $n_{\text{eff},2}$ at the wavelength λ. Therefore, it is crucial that the nano-spike radius reduce as gradually as possible to ensure that the nano-spike length is sufficient to minimise losses, while maximizing the coupling to the waveguide.

In our setup, the width of the silicon inverted taper waveguide varies from $280\,\text{nm}$ to $500\,\text{nm}$ over a distance of $30\,\mu\text{m}$. Figure 1(a) shows the effective refractive index of the silicon waveguide as a function of its width, obtained through a 2D finite element simulation. From this simulation, we determined that the optimal nano-spike radius to match the silicon waveguide is approximately $800\,\text{nm}$. Consequently, we need to developed a fabrication procedure that allows precise control over the length and radius of the nano-spike

III. Chemical Etching of the Fiber

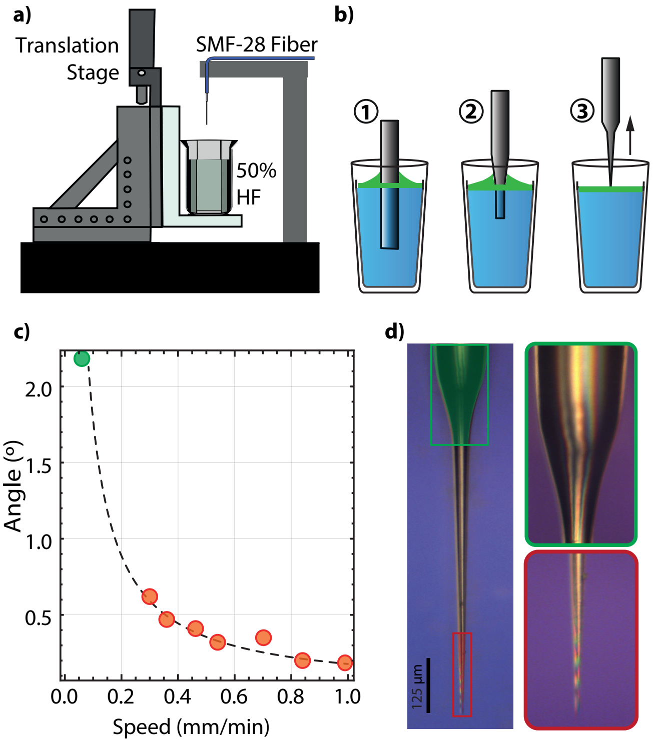

Fig. 2. **a)** Chemical etching setup for fabricating tapered fibers. **b)** Schematic of the three main stages in the etching process: 1) Lowering the fiber into an HF beaker, forming a meniscus at the HF-*Oxylene*-air interfaces; 2) Rapid conic profiling; and 3) Adiabatic tapering by slowly withdrawing the fiber from the acid. **c)** Tapering angles as a function of the withdrawal speed, with the dashed line representing the expected tapering angle for an etching rate of $1.55\,\mu\text{m}/\text{min}$. The angle of the tapered optical fiber used in this work is shown in green. **d)** Magnified images of the optical taper, highlighting the rapid transition region (green) and coupling region (red).

To produce the nano-spike with controllable dimensions, we set up an apparatus with a motorized translation stage that controls the movement of a beaker containing a solution of water and hydrofluoric acid (H_2O/HF - 50%/50%) (Fig.2(a)). The optical fiber is first immersed in the HF solution to a depth h. The surface of the acid solution is then covered with *o-xylene* oil, forming a meniscus around the fiber (Fig.2(b)). This oil layer prevents HF vapors from reaching the upper region of the fiber, which could otherwise cause surface roughness along its entire length. The fiber remains static for 30 minutes, which causes a rapid radius transition, driven by the gradual fall of the meniscus height—a phenomenon directly related to the fiber radius. With an etching rate of $1.55\,\mu\text{m}/\text{min}$ on each side, the fiber radius is then reduced to $16\,\mu\text{m}$. This rapid decrease is not contradictory to the adiabaticity criteria, since during this stage only the cladding is remove maintaining the fiber core intact.

The fiber is then pulled at a constant speed v for 10 minutes, reducing the radius to approximately $500\,\text{nm}$, a value sufficient to ensure efficient coupling with the silicon waveguide. The pulling speed determines the final length L_{taper} and the taper angle θ.

By employing this straightforward procedure, a simple relationship can be derived [5], [8] between the pulling speed v of the fiber and the resulting nano-spike tip angle θ:

$$\tan\left(\frac{\theta}{2}\right) = \frac{R}{v \cdot \tau} \tag{2}$$

This relationship allows for precise prediction of the final tip angle θ by adjusting the pulling speed v, the etching time τ, and knowing the initial fiber radius R. Fig. 2(c) shows a series of nano-spike angles retrieved from fabricated samples using this technique, demonstrating good agreement with this simple model. Using a pulling speed of $1.0\,\mu\text{m}/\text{s}$, we could then fabricate a nano-spike with the optimal geometry for the efficient coupling with the device. A micrograph of such taper is shown in Fig. 2(d).

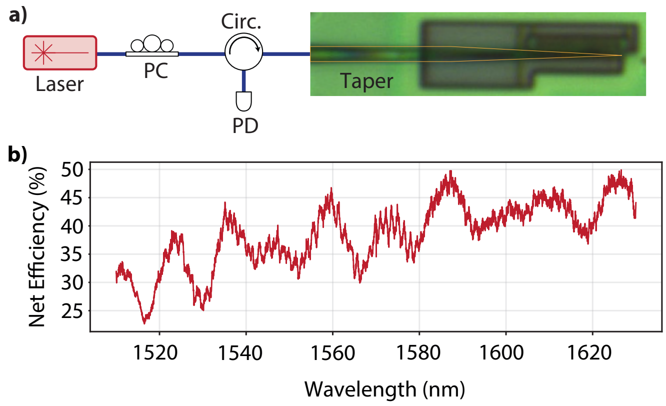

Fig. 3. **a)** Coupling efficiency characterization setup. An optical image of tapered fiber coupled to the device used in this work is shown. PC: Polarization controller; PD: Photodetector; Circ: Optical circulator. **b)** Measured total efficiency in the C-Band. The reported values are a lower bound to the fiber-waveguide efficiency coupling as the fiber optical losses are still unknown.

IV. Coupling Efficiency

To test the coupling efficiency, we measure the reflected signal from the silicon device using the setup shown in Fig.3(a). A polarization controller (PC) adjusts the light from the tunable laser to ensure efficient coupling into the guided mode of the silicon waveguide. The reflected signal from the photonic crystal waveguide is collected using a circulator (Circ.) and a photodetector (PD).

We use a XYZ-motorized stage to precisely position the nano-spike in contact with the waveguide. A microscope equipped with a camera helps us accurately align the nano-spike above the inverted taper while moving it along the waveguide to find the optimal position for the best refractive index match.

Once the nanospike is properly aligned, we perform a wavelength sweep with the laser, while measuring the reflected signal from the waveguide, to identify resonance modes of the optomechanical cavity. This allows for a fine-tune of the polarization by maximizing the coupling efficiency to the optical cavity mode.

Considering the coupling efficiency and losses in the system, we can derive the overall transmission efficiency (η_{total}) as:

$$\eta_{\text{total}} = \eta_{23} \times [(1 - \alpha_{\text{spike}}) \times \eta_{\text{coupling}}]^2 \tag{3}$$

where η_{23} represents the transmission efficiency between ports 2 and 3 of the circulator, α_{spike} denotes the transmission losses of the nano-spike, and η_{coupling} refers to the nano-spike to waveguide coupling efficiency. Both the nano-spike losses (α_{spike}) and the coupling efficiency (η_{coupling}) must be accounted for during both the in-coupling and out-coupling processes of the waveguide. η_{23} is independently measured and is equal to $0.2\,\text{dB}$. The net efficiency, which accounts for both the nano-spike losses and the coupling efficiency, is shown in Fig. 3(b) and can vary between 25% and 50%.

This is, however, a lower bound for the nano-spike-to-waveguide coupling efficiency, since we need to measure the nano-spike losses to retrieve this efficiency. This is a challenging task, as measuring these losses would require ultimately evaluating the adiabatic criterion and assessing any scattering losses due to surface roughness. Preliminary results indicate that the nano-spike losses could be as large as $\alpha_{\text{spike}} = -4\,\text{dB}$, which would result in a coupling efficiency of $\eta_{\text{coupling}} \approx 83\%$ for the lowest net coupling efficiency of 25%.

V. Conclusions

We have successfully developed a straightforward method for fabricating nanospikes designed to couple with silicon integrated waveguides. Using the fabricated probe, we obtained transmission data from the reflected signal of the target device, yielding a lower-bound single-pass coupling efficiency of over 25%. Further investigation into the nanospike losses and design could potentially lead to near-unitary coupling in the C-band, which is crucial for high-fidelity experiments.

References

[1] W. Bogaerts, D. Taillaert, B. Luyssaert, P. Dumon, J. V. Campenhout, P. Bienstman, D. V. Thourhout, R. Baets, V. Wiaux, and S. Beckx, "Basic structures for photonic integrated circuits in silicon-on-insulator," *Optics Express*, vol. 12, p. 1583, 4 2004.

[2] H. J. Kimble, "The quantum internet," *Nature*, vol. 453, pp. 1023–1030, 6 2008.

[3] T. Birks and Y. Li, "The shape of fiber tapers," *Journal of Lightwave Technology*, vol. 10, pp. 432–438, 4 1992.

[4] P. Sanchis, P. Bienstman, B. Luyssaert, R. Baets, and J. Marti, "Analysis of butt coupling in photonic crystals," *IEEE Journal of Quantum Electronics*, vol. 40, pp. 541–550, 5 2004.

[5] L. H. Haber, R. D. Schaller, J. C. Johnson, and R. J. Saykally, "Shape control of near-field probes using dynamic meniscus etching," *Journal of Microscopy*, vol. 214, pp. 27–35, 4 2004.

[6] T. G. Tiecke, K. P. Nayak, J. D. Thompson, T. Peyronel, N. P. de Leon, V. Vuletić, and M. D. Lukin, "Efficient fiber-optical interface for nanophotonic devices," *Optica*, vol. 2, p. 70, 2 2015.

[7] J. Love, W. Henry, W. Stewart, R. Black, S. Lacroix, and F. Gonthier, "Tapered single-mode fibres and devices. part 1: Adiabaticity criteria," *IEE Proceedings J Optoelectronics*, vol. 138, p. 343, 1991.

[8] Z. Wang, "Optomechanically coupled nanospike array fabricated on the endface of a soft-glass photonic crystal fiber," 2020.